

Stability and Control of Relative Equilibria for the Three-Spacecraft Coulomb Tether Problem

Islam I. Hussein and Hanspeter Schaub

Simulated Reprint from

Acta Astronautica

Vol. 65, No. 5–6, 2009, pp. 738–754

Stability and Control of Relative Equilibria for the Three-Spacecraft Coulomb Tether Problem

H. Schaub

*Aerospace Engineering Sciences Department, Colorado Center for Astrodynamics Research, University of Colorado
Boulder, CO 80309-0431.*

I. Hussein

Mechanical Engineering, Worcester Polytechnic Institute, Worcester, MA 01609.

Abstract

This paper studies the stability and control of relative equilibria for the spinning three-craft Coulomb tether problem. General conditions are derived whose solutions are all relative equilibria for the spinning charged three-craft cluster. In particular, the collinear three-craft spinning family of solutions are derived. Routhian reduction is used to employ the conservation of angular momentum to simplify the equations of motion of the system and, hence, restricting the analysis to its internal shape dynamics. This paper mainly focuses on symmetric Coulomb-tether systems, where all three craft have the same mass and nominal charge values. Based on a linearized analysis, the uncontrolled symmetric three-craft Coulomb tether system is shown to be unstable. Linear feedback control based on the linearized equations are derived to control the nonlinear dynamics of the system. The closed-loop system converges to a neighborhood of the desired equilibrium in general. If the initial condition is chosen such that the system angular momentum is equivalent to that of the desired equilibrium, asymptotic convergence is achieved.

Key words: Three-satellite Coulomb tether formations, relative equilibria, stability and control.

1. Introduction

Recent research has begun to investigate exploiting the naturally occurring electrostatic forces of spacecraft operating High Earth Orbits (HEO) or deep space. The NIAC study performed by King et al. (2002) illustrates that the absolute spacecraft charges can reach kilo-volt levels at GEO. This results in micro- to milli-Newton levels of disturbance forces if the craft are flying

Email addresses: hanspeter.schaub@colorado.edu (H. Schaub), ihussein@wpi.edu (I. Hussein).

dozens of meters apart. Over an orbit, this disturbance can cause hundreds of meters of error motion. The Coulomb thrusting concept proposes to use active charge control to servo the absolute spacecraft charge levels to desired values and exploit this disturbance force to perform direct relative motion control (Schaub et al., 2004; King et al., 2003). The electrostatic charge of a craft is partially masked from another nearby craft due to the interaction with the space plasma ions and electrons. The strength of this shielding is measured through the Debye length (Nicholson, 1992; Gombosi, 1998). The cold and dense plasma environment at Low Earth Orbits (LEO) causes the Debye lengths to be of the order of centimeters, making Coulomb thrusting over dozens of meters separation distances infeasible. At Geostationary Earth Orbits (GEO) the Debye length can range between 100-1000 meters, making it feasible to exploit Coulomb thrusting (King et al., 2002; Romanelli et al., 2006). At 1 AU distance from the sun the deep space Debye lengths range between 30-50 meters (King et al., 2002).

Close proximity flying on the order of dozens of meters is very challenging due to the large number of small orbit corrections that must be performed to avoid collisions and maintain a desired relative orbit geometry. Further, exhaust plume impingement issues must be addressed to avoid having one spacecraft fire in the direction of a neighboring spacecraft. The Coulomb thrusting typically only requires Watt levels of electrical power, while consuming essentially no fuel. I_{sp} fuel efficiencies range between $10^9 - 10^{12}$ seconds (King et al., 2002; Lappas et al., 2007). Spacecraft charge control has been demonstrated on the earlier SCATHA (Mullen et al., 1986) and ATS (Whipple and Olsen, 1980) missions, as well as more recently by the European CLUSTERS mission (Escoubet et al., 2001; Torkar and et. al., 1999). With CLUSTERS the absolute spacecraft potential is controlled to near zero relative to the plasma ground to avoid biasing the particle sensors.

The Coulomb thrusting research has led to a multitude of novel relative motion missions. The concept of virtual Coulomb structures has open-loop electrostatic forces perfectly cancel out the differential gravitational acceleration, resulting in a spacecraft cluster whose satellite positions appear frozen as seen by the rotating chief local-vertical-local-horizontal (LVLH) frame (King et al., 2002; Schaub et al., 2005; Berryman and Schaub, 2005a,b). However, all charged *static* relative equilibria solutions in orbit or in deep space have been unstable and will require active charge feedback to stabilize.

The first feedback stabilized charged virtual structures is the 2-craft Coulomb tether concept discussed by Natarajan and Schaub (2006), Natarajan et al. (2006) and Natarajan and Schaub (2007). While a physical tether must always be in tension, the Coulomb tether can exert both attractive and repulsive forces between the 2 craft. However, the Coulomb tether concept is only viable for relatively short separation distances up to 100 meters, while the typical space tether concepts consider kilometer size tether lengths.

Both of these Coulomb mission concepts consider static scenarios where the craft are at nominally fixed locations relative to a reference frame (orbit frame). More recently the feasibility of spinning charged spacecraft formations has been considered. Hussein and Schaub (2006a) investigate the similarity between the gravitational and electrostatic spinning 3-body problem to determine invariant shape solutions. Lagrange's treatment of the gravitational 3-body problem is applied to the electro-static 3-body problem to develop collinear and equilateral triangle solutions, as well as discuss the boundedness of these motions. However, the stability of these solutions is not addressed in this paper.

The first passively stable virtual Coulomb structure is the spinning 2-craft system discussed by Schaub and Hussein (2007). Without the plasma charge shielding effect, the attractive force between two oppositely charged bodies is mathematically equivalent to the gravitational 2-body

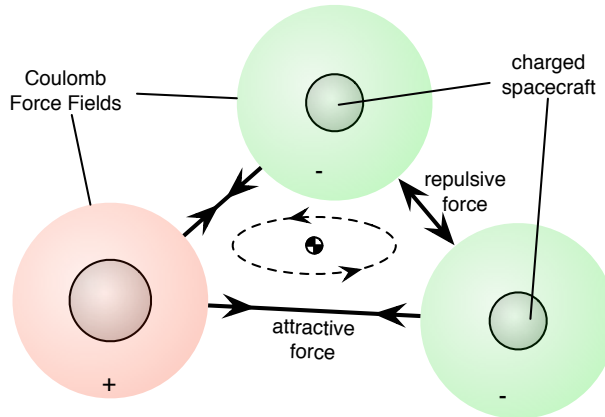


Fig. 1. Illustration of a 3-craft Coulomb spacecraft formation spinning in deep space about their cluster center of mass.

force. The resulting trajectories of the 2 craft are also conic solutions which are orbitally stable. With the finite Debye lengths and charge shielding included, the relative trajectories are no longer closed conic solutions. Rather, the charge shielding causes an additional weakening of the attractive force. Schaub and Hussein (2007) show that if the nominal circular relative motion has a radius less than the Debye length, then the resulting nonlinear motion is still stable.

While Hussein and Schaub (2006a) investigate invariant shape solutions to the spinning charged 3-craft problem illustrated in Figure 1, this paper studies the general relative equilibriums of such a system, as well as discuss the open-loop stability. Energy-momentum methods are employed to study the complex dynamical system where charge shielding is included through a finite Debye length value. Close flying spinning multi-craft systems can be used for interested distributed interferometry missions such as the terrestrial planet finder concepts. The charged spacecraft are assumed to be flying on circular heliocentric orbits, far removed from the gravitational potential fields of planets or other celestial bodies. Thus this study can neglect the relative gravitational forces and focus on the motion of free-flying bodies due to the electrostatic forces.

2. The Three-Craft Constellation

2.1. Invariance of the Hamiltonian

Consider a spacecraft cluster composed of three charged craft operating in deep space. Thus the orbital dynamics are ignored in this development. However, the plasma shielding effect is included with a finite Debye length. At 1 AU the Debye length can range between 30–50 meters due to the solar flux (King et al., 2002). The craft have masses m_1 , m_2 and m_3 and charges c_1 , c_2 and c_3 , respectively. The inertial positions of the three craft are denoted by \mathbf{r}_1 , \mathbf{r}_2 , and \mathbf{r}_3 . The total system kinetic energy is given by

$$\begin{aligned} K(\mathbf{r}_1, \mathbf{r}_2, \mathbf{r}_3, \dot{\mathbf{r}}_1, \dot{\mathbf{r}}_2, \dot{\mathbf{r}}_3) \\ = \frac{1}{2} \left(m_1 \|\dot{\mathbf{r}}_1\|^2 + m_2 \|\dot{\mathbf{r}}_2\|^2 + m_3 \|\dot{\mathbf{r}}_3\|^2 \right), \end{aligned} \quad (1)$$

where $\|\cdot\|$ denotes the Euclidean norm in \mathbb{R}^3 .

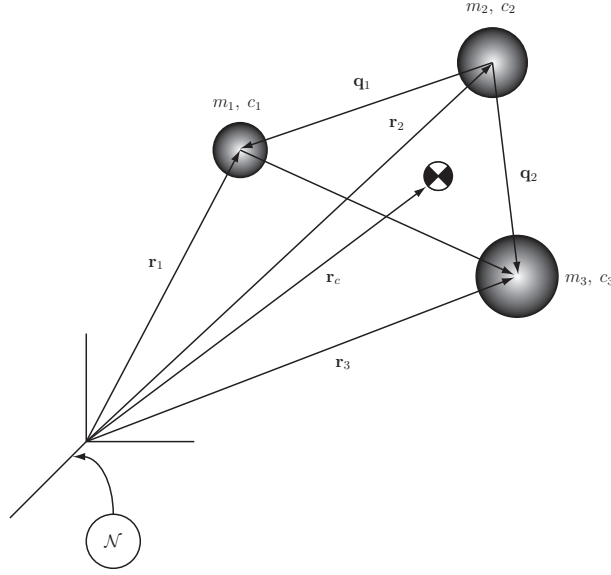


Fig. 2. The three-craft Coulomb tether system.

Let $\mathbf{q}_1 = \mathbf{r}_1 - \mathbf{r}_2$, $\mathbf{q}_2 = \mathbf{r}_3 - \mathbf{r}_2$ and $\mathbf{q}_c = \frac{m_1\mathbf{r}_1 + m_2\mathbf{r}_2 + m_3\mathbf{r}_3}{m_1 + m_2 + m_3}$ be the relative position vector between the first and second spacecraft, the relative position vector between the second and third spacecraft, and the system center of mass vector. We will fix the center of mass with $\mathbf{q}_c = 0$. This is equivalent to restricting the system motion to the zero linear momentum surface.

In terms of \mathbf{q}_1 and \mathbf{q}_2 , the kinetic energy is then given by

$$\begin{aligned}
 K(\mathbf{q}_1, \mathbf{q}_2, \dot{\mathbf{q}}_1, \dot{\mathbf{q}}_2) &= \frac{1}{2} \left(\frac{m_1(m_2 + m_3)}{M} \|\dot{\mathbf{q}}_1\|^2 + \frac{m_3(m_2 + m_1)}{M} \|\dot{\mathbf{q}}_2\|^2 \right. \\
 &\quad \left. - \frac{2m_1m_3}{M} \dot{\mathbf{q}}_1 \cdot \dot{\mathbf{q}}_2 \right), \tag{2}
 \end{aligned}$$

where $M = m_1 + m_2 + m_3$ is the total cluster mass. The potential energy V is purely due to the electrostatic charges c_1 , c_2 and c_3 , and is a function of $q_1 = \|\mathbf{q}_1\|$, $q_2 = \|\mathbf{q}_2\|$, and $q_{12} = \|\mathbf{q}_1 - \mathbf{q}_2\|$. The total cluster electrostatic potential function is given by

$$\begin{aligned}
 V(\mathbf{r}) &= \frac{\mu_{12}}{\|\mathbf{q}_1\|} e^{-\frac{\|\mathbf{q}_1\|}{\lambda_d}} - \frac{\mu_{12}}{\lambda_d} \int_{\frac{\|\mathbf{q}_1\|}{\lambda_d}}^{\infty} \frac{e^{-s}}{s} ds + \frac{\mu_{23}}{\|\mathbf{q}_2\|} e^{-\frac{\|\mathbf{q}_2\|}{\lambda_d}} \\
 &\quad - \frac{\mu_{23}}{\lambda_d} \int_{\frac{\|\mathbf{q}_2\|}{\lambda_d}}^{\infty} \frac{e^{-s}}{s} ds + \frac{\mu_{13}}{\|\mathbf{q}_1 - \mathbf{q}_2\|} e^{-\frac{\|\mathbf{q}_1 - \mathbf{q}_2\|}{\lambda_d}} \\
 &\quad - \frac{\mu_{13}}{\lambda_d} \int_{\frac{\|\mathbf{q}_1 - \mathbf{q}_2\|}{\lambda_d}}^{\infty} \frac{e^{-s}}{s} ds, \tag{3}
 \end{aligned}$$

where λ_d is the Debye length which determines the strength of the electrostatic shielding of the surrounding space plasma, and

$$\mu_{12} = k_c c_1 c_2, \quad \mu_{13} = k_c c_1 c_3, \quad \mu_{23} = k_c c_2 c_3. \tag{4}$$

The Lagrangian is given by $\mathcal{L} = K - V$.

We now express the kinetic energy in terms of the momentum variables

$$\begin{aligned}\mathbf{p}_1 &= \frac{\partial \mathcal{L}}{\partial \dot{\mathbf{q}}_1} = \frac{m_1(m_2 + m_3)}{M} \dot{\mathbf{q}}_1 - \frac{m_1 m_3}{M} \dot{\mathbf{q}}_2 \\ \mathbf{p}_2 &= \frac{\partial \mathcal{L}}{\partial \dot{\mathbf{q}}_2} = \frac{m_3(m_2 + m_1)}{M} \dot{\mathbf{q}}_2 - \frac{m_1 m_3}{M} \dot{\mathbf{q}}_1.\end{aligned}\quad (5)$$

The kinetic energy is given by

$$\begin{aligned}K(\mathbf{q}_1, \mathbf{q}_2, \mathbf{p}_1, \mathbf{p}_2) &= \frac{1}{2} \left(\frac{(m_1 + m_2)}{m_1 m_2} \|\mathbf{p}_1\|^2 \right. \\ &\quad \left. + \frac{(m_2 + m_3)}{m_2 m_3} \|\mathbf{p}_2\|^2 + \frac{2}{m_2} \mathbf{p}_1 \cdot \mathbf{p}_2 \right),\end{aligned}\quad (6)$$

with the Hamiltonian given by

$$H(\mathbf{q}_1, \mathbf{q}_2, \mathbf{p}_1, \mathbf{p}_2) = K(\mathbf{q}_1, \mathbf{q}_2, \mathbf{p}_1, \mathbf{p}_2) + V(\mathbf{q}_1, \mathbf{q}_2). \quad (7)$$

We now consider the action of the rotation group $\text{SO}(3)$, which corresponds to a rigid body rotation of the two-craft formation (Marsden and Ratiu, 1999):

$$\Psi_{\mathbf{R}}(\mathbf{q}_1, \mathbf{q}_2) = \Psi(\mathbf{R}, \mathbf{q}_1, \mathbf{q}_2) = (\mathbf{R}\mathbf{q}_1, \mathbf{R}\mathbf{q}_2), \quad (8)$$

for all $\mathbf{R} \in \text{SO}(3)$, with the corresponding lifted action

$$T\Psi_{\mathbf{R}}(\mathbf{q}_1, \mathbf{q}_2, \dot{\mathbf{q}}_1, \dot{\mathbf{q}}_2) = (\mathbf{R}\mathbf{q}_1, \mathbf{R}\mathbf{q}_2, \mathbf{R}\dot{\mathbf{q}}_1, \mathbf{R}\dot{\mathbf{q}}_2). \quad (9)$$

This lifted action is on the tangent space (i.e., space of configurations and velocities). This lifted action says that under a rigid body rotation of the entire system, the rate of change of \mathbf{q} has to be rotated exactly by the rotation matrix \mathbf{R} in order to preserve the shape of the formation. The action on the space of momenta is denoted by $T^*\Psi_{\mathbf{R}}$ and is given by:

$$T^*\Psi_{\mathbf{R}}(\mathbf{q}_1, \mathbf{q}_2, \mathbf{p}_1, \mathbf{p}_2) = (\mathbf{R}\mathbf{q}_1, \mathbf{R}\mathbf{q}_2, \mathbf{R}\mathbf{p}_1, \mathbf{R}\mathbf{p}_2). \quad (10)$$

The Hamiltonian is invariant with respect to the action of the rotational group $\text{SO}(3)$ action (i.e., $H(T^*\Psi_{\mathbf{R}}(\mathbf{q}_1, \mathbf{q}_2, \mathbf{p}_1, \mathbf{p}_2)) = H(\mathbf{R}\mathbf{q}_1, \mathbf{R}\mathbf{q}_2, \mathbf{R}\mathbf{p}_1, \mathbf{R}\mathbf{p}_2) = H(\mathbf{q}_1, \mathbf{q}_2, \mathbf{p}_1, \mathbf{p}_2)$). This is easy to verify because $\|\mathbf{R}\mathbf{p}_i\|^2 = \|\mathbf{p}_i\|^2$ and $\|\mathbf{R}\mathbf{q}_i\|^2 = \|\mathbf{q}_i\|^2$ (noting that V is a function of the magnitude of its argument), and $\mathbf{R} \in \text{SO}(3)$ is an orthonormal matrix. This invariance implies that there is a conserved quantity $\mathbf{J}_{\text{SO}(3)}$, called the momentum map, associated with action of $\text{SO}(3)$. It can be shown that this conserved quantity is given by (see Marsden and Ratiu (1999))

$$\mathbf{J}_{\text{SO}(3)} = \mathbf{q}_1 \times \mathbf{p}_1 + \mathbf{q}_2 \times \mathbf{p}_2, \quad (11)$$

which is the angular momentum of the system. This momentum is conserved if the system is not actuated by any external forces.

2.2. Relative Equilibria

To obtain expressions for relative equilibria of the system, we first need to compute the locked inertia tensor, which is a map $\mathbb{I}(\mathbf{q}) : \mathfrak{so}(3) \rightarrow \mathfrak{so}^*(3)$, where $\mathfrak{so}(3)$ is the $\text{SO}(3)$ Lie algebra (the

algebra of spatial ‘‘twists’’). This tensor is the inertia of the system if its shape coordinates are locked as if the system is a rigid body. The locked inertia tensor is given by

$$\langle \mathbb{I}(\mathbf{q})\boldsymbol{\eta}, \boldsymbol{\xi} \rangle = \ll \boldsymbol{\eta}_{\text{SO}(3)}, \boldsymbol{\xi}_{\text{SO}(3)} \gg,$$

for all $\boldsymbol{\eta}, \boldsymbol{\xi} \in \mathfrak{so}(3)$, and where $\ll \cdot, \cdot \gg$ denotes the kinetic energy metric. $\boldsymbol{\xi}_{\text{SO}(3)}$ denotes the infinitesimal generator associated with the action of $\text{SO}(3)$. The infinitesimal generator of an action is the infinitesimal description of an action. It is a velocity vector (in this case an angular velocity vector) that completely describes how the action transforms a configuration while the shape of the system is maintained. The infinitesimal generator for the $\text{SO}(3)$ group action is simply given by the cross product: $\boldsymbol{\xi}_{\text{SO}(3)}(\mathbf{q}_1, \mathbf{q}_2) = (\mathbf{q}_1, \mathbf{q}_2, \boldsymbol{\xi} \times \mathbf{q}_1, \boldsymbol{\xi} \times \mathbf{q}_2)$, which acts at the configuration $(\mathbf{q}_1, \mathbf{q}_2)$ and to induce a velocity vector $(\boldsymbol{\xi} \times \mathbf{q}_1, \boldsymbol{\xi} \times \mathbf{q}_2)$. The infinitesimal generator in this case is simply given by taking the cross product of the angular velocity variable $\boldsymbol{\xi} \in \mathfrak{so}(3)$ with the configuration variables $\mathbf{q}_1, \mathbf{q}_2$. Under such an operation the system is transformed to a new configuration that has exactly the same shape as that before application of the action $\Psi_{\mathbf{R}}$. In this case it represents a pure net change in orientation while the shape is preserved.

Using the above definition for the locked inertia, one can find that the locked inertia tensor is given by:

$$\begin{aligned} \mathbb{I}(\mathbf{q}_1, \mathbf{q}_2) &= \frac{m_1(m_2 + m_3)}{M} \left(\|\mathbf{q}_1\|^2 \text{Id} - \mathbf{q}_1 \otimes \mathbf{q}_1 \right) \\ &\quad + \frac{m_3(m_2 + m_1)}{M} \left(\|\mathbf{q}_2\|^2 \text{Id} - \mathbf{q}_2 \otimes \mathbf{q}_2 \right) \\ &\quad - \frac{m_1 m_3}{M} (2(\mathbf{q}_1 \cdot \mathbf{q}_2) \text{Id} - \mathbf{q}_1 \otimes \mathbf{q}_2 - \mathbf{q}_2 \otimes \mathbf{q}_1), \end{aligned} \quad (12)$$

where $\text{Id} : \mathfrak{so}^*(3) \rightarrow \mathfrak{so}^*(3)$ is the identity operator and $\mathbf{q}_i \otimes \mathbf{q}_j$ is often denoted as the dyadic $\mathbf{q}_i \mathbf{q}_j$.

The augmented augmented potential function $V_{\boldsymbol{\xi}}$ is defined by

$$\begin{aligned} V_{\boldsymbol{\xi}} &= V(\mathbf{q}_1, \mathbf{q}_2) - \frac{1}{2} \langle \boldsymbol{\xi}, \mathbb{I}(\mathbf{q}_1, \mathbf{q}_2) \boldsymbol{\xi} \rangle \\ &= V(\mathbf{q}_1, \mathbf{q}_2) - \frac{1}{2M} \left\{ [m_1(m_2 + m_3) \|\mathbf{q}_1\|^2 \right. \\ &\quad + m_3(m_1 + m_2) \|\mathbf{q}_2\|^2 - 2m_1 m_3 \mathbf{q}_1 \cdot \mathbf{q}_2] \|\boldsymbol{\xi}\|^2 \\ &\quad - m_1(m_2 + m_3) (\mathbf{q}_1 \cdot \boldsymbol{\xi})^2 - m_3(m_1 + m_2) (\mathbf{q}_2 \cdot \boldsymbol{\xi})^2 \\ &\quad \left. + 2m_1 m_3 (\mathbf{q}_1 \cdot \boldsymbol{\xi})(\mathbf{q}_2 \cdot \boldsymbol{\xi}) \right\} \end{aligned} \quad (13)$$

can be used to determine the relative equilibria (Marsden, 1992).

A point in the cotangent space $(\mathbf{q}_{1e}, \mathbf{q}_{2e}, \mathbf{p}_{1e}, \mathbf{p}_{2e})$ is a relative equilibrium of the system if and only if there is a $\boldsymbol{\xi}$ such that $(\mathbf{p}_{1e}, \mathbf{p}_{2e}) = \mathbb{F}L(\boldsymbol{\xi}_{\text{SO}(3)})$ and $(\mathbf{q}_{1e}, \mathbf{q}_{2e})$ is a critical point of $V_{\boldsymbol{\xi}}(\mathbf{q}_1, \mathbf{q}_2)$ (Marsden, 1992). In the present case, this means that a point in phase space is a relative equilibrium if there is a velocity $\boldsymbol{\xi}$ such that satisfy:

$$\begin{aligned}
0 &= -\frac{\mu_{12}e^{-\|\mathbf{q}_1\|/\lambda_d}}{\|\mathbf{q}_1\|^3}\mathbf{q}_1 - \frac{\mu_{13}e^{-\|\mathbf{q}_1-\mathbf{q}_2\|/\lambda_d}}{\|\mathbf{q}_1-\mathbf{q}_2\|^3}(\mathbf{q}_1-\mathbf{q}_2) \\
&\quad -\frac{1}{M}\left[m_1(m_2+m_3)\boldsymbol{\xi}\times(\mathbf{q}_1\times\boldsymbol{\xi})\right. \\
&\quad \left.-m_1m_3\boldsymbol{\xi}\times(\mathbf{q}_2\times\boldsymbol{\xi})\right] \\
0 &= -\frac{\mu_{23}e^{-\|\mathbf{q}_2\|/\lambda_d}}{\|\mathbf{q}_2\|^3}\mathbf{q}_2 + \frac{\mu_{13}e^{-\|\mathbf{q}_1-\mathbf{q}_2\|/\lambda_d}}{\|\mathbf{q}_1-\mathbf{q}_2\|^3}(\mathbf{q}_1-\mathbf{q}_2) \\
&\quad -\frac{1}{M}\left[m_3(m_1+m_2)\boldsymbol{\xi}\times(\mathbf{q}_2\times\boldsymbol{\xi})\right. \\
&\quad \left.-m_1m_3\boldsymbol{\xi}\times(\mathbf{q}_1\times\boldsymbol{\xi})\right] \\
\mathbf{p}_{1e} &= \frac{m_1(m_2+m_3)}{M}\boldsymbol{\xi}\times\mathbf{q}_{1e} - \frac{m_1m_3}{M}\boldsymbol{\xi}\times\mathbf{q}_{2e} \\
\mathbf{p}_{2e} &= \frac{m_3(m_1+m_2)}{M}\boldsymbol{\xi}\times\mathbf{q}_{2e} - \frac{m_1m_3}{M}\boldsymbol{\xi}\times\mathbf{q}_{1e}.
\end{aligned}$$

The above conditions represent sufficient conditions for the existence of relative equilibria, which in the present case are spinning three-craft configurations. These conditions are nonlinear and very difficult to solve. However, one can check for example that collinear solutions do exist. In previous work, the authors solved for shape preserving three-craft constellations, which include circularly spinning three-craft relative equilibria (Hussein and Schaub, 2006b). In that work, one had to solve a quintic nonlinear equation and then for the spin rate $\boldsymbol{\xi}$. Using the method described in this paper, that relies on the geometric approaches described by Marsden (1992), the conditions given above cater solutions to the quintic equation directly.

For example, consider a three-spacecraft collinear spinning constellation. Say that we are given a desired charge on spacecraft 1 and 2, and given desired separation distances q_{e1} and q_{e2} . The above conditions when evaluated at these equilibrium values become linear algebraic equations in the charge c_3 of the third spacecraft and in the square of the magnitude of the spin rate $\boldsymbol{\xi}$. Solving for c_3 and $\xi^2 = \|\boldsymbol{\xi}\|^2$, one obtains

$$c_3 = \frac{c_1c_2e^{(q_{e2}/\lambda_d)}m_3q_{e2}^2(q_{e1}+q_{e2})^2(m_2q_{e2}+m_1(q_{e1}+q_{e2}))}{q_{e1}^2(c_1m_2q_{e2}^2(m_1q_{e1}-m_3q_{e2})+c_2e^{(q_{e1}/\lambda_d)}m_1(q_{e1}+q_{e2})^2(m_2q_{e1}+m_3(q_{e1}+q_{e2})))} \quad (14)$$

and

$$\xi = \sqrt{\frac{-c_1c_2e^{(-q_{e1}/\lambda_d)}k_cM(c_1q_{e2}^2+c_2e^{(q_{e1}/\lambda_d)}(q_{e1}+q_{e2})^2)}{(q_{e1}^2(c_1m_2q_{e2}^2(m_1q_{e1}-m_3q_{e2})+c_2e^{(q_{e1}/\lambda_d)}m_1(q_{e1}+q_{e2})^2(m_2q_{e1}+m_3(q_{e1}+q_{e2}))))}}. \quad (15)$$

Hence, we see that for an equilibrium c_1 and c_3 have to be of the same sign (from equation (14)) and that c_2 has to be opposite to both c_1 and c_3 (from equation (15)). One can check that the above value for c_3 solves the quintic equation derived by Hussein and Schaub (2006b). The advantage of the above approach is that the quintic equations is readily solved, along with the desired spin rate ξ .

One can see that there is a large family of collinear spinning three spacecraft solutions. The above solution (equations (43) and (44)) completely describe the entire family of collinear solutions. One can then use the energy omentum method to determine the stability conditions needed for a stable spinning three craft problem.

3. Formation Shape Instability with Equilibrium Charges

Unlike the charged spinning two-craft problem discussed by Schaub and Hussein (2007), under no condition is the circular trajectory relative equilibrium of the three-craft problem stable without a charge feedback control law. By means of linearization of the second order dynamics of the formation, we will show that the system is unstable. For the perfectly symmetric case (i.e., three craft with identical masses and equally spaced craft), this will be proven analytically. For the general nonsymmetric formation, instability will be shown numerically since the resulting equations are far too complex.

3.1. The Reduced Equations of Motion

So far we have not written down the equations of motion. We do so in this section using Routhian reduction. The Lagrangian for this system is given by $\mathcal{L} = K - V$, where K and V are expressed in Eqs. (2) and (3). We have so far not used any specific coordinate definition for \mathbf{q}_1 and \mathbf{q}_2 . To simplify the analysis we will assume a planar formation. In this case, we use the following coordinates: $q_1 = |\mathbf{q}_1| = |\mathbf{r}_1 - \mathbf{r}_2|$ is the relative distance between vehicles 1 and 2, $q_2 = |\mathbf{q}_2| = |\mathbf{r}_3 - \mathbf{r}_2|$ is the relative distance between vehicles 2 and 3, θ_1 is the angle between the vector \mathbf{q}_1 and an inertial x-axis, and θ_2 is the angle between \mathbf{q}_2 and \mathbf{q}_1 .

With this definition for a coordinate system, one can easily verify that $\frac{\partial \mathcal{L}}{\partial \theta_1} = 0$ and, hence, the (angular) momentum associated with θ_1 , p_{θ_1} , is conserved: $\dot{p}_{\theta_1} = 0$ (this is easily checked from the Euler-Lagrange equation for θ_1). Routh reduction (Marsden, 1992) is a procedure that uses conservation of momenta variables to reduce the size of the resulting equations. In the present case, the value of p_{θ_1} is set to a constant value h determined by the initial conditions. Obtaining an expression for p_{θ_1} from the fact that

$$\begin{aligned} h = p_{\theta_1} &= \frac{\partial \mathcal{L}}{\partial \dot{\theta}_1} \\ &= \frac{1}{M} \left((m_1 + m_2)m_3 \left(\dot{\theta}_1 + \dot{\theta}_2 \right) q_2^2 \right. \\ &\quad \left. + m_1 m_3 \left(\sin \theta_2 \dot{q}_1 - \cos \theta_2 q_1 \left(2\dot{\theta}_1 + \dot{\theta}_2 \right) \right) q_2 \right. \\ &\quad \left. + m_1 q_1 \left((m_2 + m_3) q_1 \dot{\theta}_1 - m_3 \sin \theta_2 \dot{q}_2 \right) \right). \end{aligned}$$

Using this expression to solve for $\dot{\theta}_1$, one obtains

$$\dot{\theta}_1 = \frac{hM + m_1 m_3 \sin \theta_2 (q_1 \dot{q}_2 - q_2 \dot{q}_1) - m_3 q_2 ((m_1 + m_2) q_2 - m_1 \cos \theta_2 q_1) \dot{\theta}_2}{m_1 (m_2 + m_3) q_1^2 - 2m_1 m_3 \cos \theta_2 q_2 q_1 + (m_1 + m_2) m_3 q_2^2}. \quad (16)$$

Eq. (16) is then used to remove $\dot{\theta}_1$ in

$$\mathcal{L}(q_1, q_2, \theta_1, \theta_2, \dot{q}_1, \dot{q}_2, \dot{\theta}_1, \dot{\theta}_2) - h\dot{\theta}_1$$

to obtain the Routhian $\mathcal{R}(q_1, q_2, \theta_1, \theta_2, \dot{q}_1, \dot{q}_2, \dot{\theta}_2)$.

The equations of motion of the three-craft system are obtained from the Euler-Lagrange equations, but with the Lagrangian replaced with the Routhian. One can reconstruct the solution for

θ_1 using equation (16). The equations of motion for q_1, q_2, θ_2 are given by (we omit the detailed expressions due to their length):

$$\begin{aligned}\frac{d}{dt} \frac{\partial \mathcal{R}}{\partial q_1} - \frac{\partial \mathcal{R}}{\partial q_1} &= 0 \\ \frac{d}{dt} \frac{\partial \mathcal{R}}{\partial q_2} - \frac{\partial \mathcal{R}}{\partial q_2} &= 0 \\ \frac{d}{dt} \frac{\partial \mathcal{R}}{\partial \theta_2} - \frac{\partial \mathcal{R}}{\partial \theta_2} &= 0.\end{aligned}\tag{17}$$

3.2. Linearized Equations of Motion

In this section we linearize the equations of motion about a nominal equilibrium solution described by $q_1 = q_{e1}, q_2 = q_{e2}, \theta_2 = \pi$ with all their derivatives equal to zero. Note that this equilibrium in the reduced space corresponds to a spinning formation with angular rate given by

$$\xi = \frac{(m_1 + m_2 + m_3)h}{m_2 m_3 q_{e2}^2 + m_1 (m_2 q_{e1}^2 + m_3 (q_{e1} + q_{e2})^2)}$$

and with $\theta_1 = \xi t$. The spacecraft charges are assumed constant in the linearization. Later, when we use the spacecraft charges as control inputs, the three charges c_1, c_2, c_3 will be treated as variable and the equations have to be linearized with respect to them as well.

Linearizing the equations of motion about the circular equilibrium solution described above one gets

$$\mathbf{A}\delta\ddot{\mathbf{x}} + \mathbf{B}\delta\dot{\mathbf{x}} + \mathbf{C}\delta\mathbf{x} = \mathbf{D}\delta h,\tag{18}$$

where the matrices $\mathbf{A}, \mathbf{B}, \mathbf{C}$ and \mathbf{D} are defined in the appendix. Note that perturbations may also cause the value of the conserved angular momentum be different from the nominal angular momentum h . For this system δh is viewed as a constant (persistent) input force. In these equation we have substituted c_3 from equation (14), h from equation (18), and where $\mathbf{x} = [q_1 \ q_2 \ \theta_2]^T$. Next we will study the stability of these linearized equations for a special case.

3.3. System Stability: Symmetric Case

In this section we will check the eigenvalues of the linearized system for the circular equilibrium of interest with $q_{1e} = q_{2e} = q_e$ (this equilibrium also implies that the nominal equilibrium charges are $c_1 = c_3 = -c_2 = c$). We will also assume that $m_1 = m_2 = m_3 = m$. To study the stability of the unactuated system, one need only study the unforced system (i.e., with $\delta h = 0$). The reasoning is as follows. If under zero error in the angular momentum h (i.e., the initial conditions are such that $\delta h = 0$) the system is stable, then due to a (constant) nonzero momentum error δh , the linearized system converges to a neighborhood of the desired relative equilibrium. The neighborhood is given by the steady state error:

$$\delta \mathbf{x}_{ss} = \mathbf{C}^{-1} \mathbf{D} \delta h.$$

If the relative equilibrium is unstable, then it is unstable for all initial conditions, whether they result in a zero or nonzero δh . Hence, if the relative equilibrium is unstable with $\delta h = 0$ for

the linearized system, then it must be unstable in general (i.e., for all other initial conditions that result in a nonzero angular momentum error δh), and so must be the original nonlinear system.

The characteristic equation is given by

$$f(s) = \det [\mathbf{A}s^2 + \mathbf{B}s + \mathbf{C}], \quad (19)$$

which is a sixth order equation with 6 roots. These roots are the system eigenvalues. In the symmetric case, the matrices \mathbf{A} , \mathbf{B} , and \mathbf{C} are given by

$$\mathbf{A} = \begin{bmatrix} \frac{2m}{3} & \frac{m}{3} & 0 \\ \frac{m}{3} & \frac{2m}{3} & 0 \\ 0 & 0 & \frac{mq_e^2}{6} \end{bmatrix},$$

$$\mathbf{B} = \begin{bmatrix} 0 & 0 & \frac{mq_e\xi}{3} \\ 0 & 0 & -\frac{mq_e\xi}{3} \\ -\frac{mq_e\xi}{3} & \frac{mq_e\xi}{3} & 0 \end{bmatrix}$$

$$\mathbf{C} = \begin{bmatrix} -\frac{c_0^2 k_c e^{-2\beta}}{4q_e^3} - \frac{m(2+3\beta)\xi^2}{3} & \frac{c_0^2 k_c e^{-2\beta}(1+\beta)}{4q_e^3} + \frac{5m\xi^2}{3} & 0 \\ \frac{c_0^2 k_c e^{-2\beta}(1+\beta)}{4q_e^3} + \frac{5m\xi^2}{3} & -\frac{c_0^2 k_c e^{-2\beta}}{4q_e^3} - \frac{m(2+3\beta)\xi^2}{3} & 0 \\ 0 & 0 & \frac{c_0^2 k_c e^{-2\beta}}{8q_e} + \frac{1}{3}mq_e^2\xi^2 \end{bmatrix}.$$

One can check that the eigenvalues are given by

$$s_{1,2} = \pm \frac{\sqrt{\alpha}\sqrt{(\beta-1)\bar{h} - e^{-2\beta}\beta}}{2mq_e^2}$$

$$s_{3,4} = \pm \frac{\sqrt{\frac{e^{-4\beta}\alpha\left(3e^{2\beta}(\beta+1)+e^{4\beta}(3\beta+1)\bar{h}-\sqrt{3}\sqrt{e^{4\beta}(e^{2\beta}\bar{h}+1)(3(\beta+3)^2+e^{2\beta}(\beta(3\beta+10)+19)\bar{h})}\right)}{m^2q_e^4}}}{2\sqrt{2}} \quad (20)$$

$$s_{5,6} = \pm \frac{\sqrt{\frac{e^{-4\beta}\alpha\left(3e^{2\beta}(\beta+1)+e^{4\beta}(3\beta+1)\bar{h}+\sqrt{3}\sqrt{e^{4\beta}(e^{2\beta}\bar{h}+1)(3(\beta+3)^2+e^{2\beta}(\beta(3\beta+10)+19)\bar{h})}\right)}{m^2q_e^4}}}{2\sqrt{2}},$$

where

$$\alpha = c^2 k_c m q_e \quad \beta = \frac{q_e}{\lambda_d} \quad \bar{h} = \frac{h^2}{\alpha}.$$

Showing that at least one of these eigenvalues is a positive real number is not easy. Instead we will show instability by studying the coefficients of the characteristic polynomial.

Letting $x = s^2$, the characteristic function can be rewritten in the cubic form

$$f(x) = a_3x^3 + a_2x^2 + a_1x + a_0. \quad (21)$$

In the above, a_3, a_2, a_1, a_0 are functions of q_e, c, m :

$$\begin{aligned} a_3 &= \frac{m^3 q_e^2}{18} \\ a_2 &= \frac{e^{-\frac{2q_e}{\lambda_d}} m \left(-16e^{\frac{q_e}{\lambda_d}} k_c m q_e (2\lambda_d + q_e) c^2 + k_c m q_e (5\lambda_d + 2q_e) c^2 + 8e^{\frac{2q_e}{\lambda_d}} h^2 \lambda_d \right)}{72\lambda_d q_e^2} \\ a_1 &= \frac{1}{288\lambda_d^2 m q_e^6} \times \\ &\quad \left(e^{-\frac{4q_e}{\lambda_d}} \left(6k_c^2 \lambda_d m^2 q_e^2 (\lambda_d + q_e) c^4 - 24e^{\frac{q_e}{\lambda_d}} k_c^2 m^2 q_e^2 (2\lambda_d + q_e) (3\lambda_d + q_e) c^4 \right. \right. \\ &\quad \left. \left. - 80e^{\frac{3q_e}{\lambda_d}} h^2 k_c \lambda_d m q_e (2\lambda_d + q_e) c^2 + 2e^{\frac{2q_e}{\lambda_d}} k_c m q_e (\lambda_d (8\lambda_d + 5q_e) h^2 \right. \right. \\ &\quad \left. \left. + 24c^2 k_c m q_e (2\lambda_d + q_e)^2 c^2 + 13e^{\frac{4q_e}{\lambda_d}} h^4 q_e^2 \right) \right) \\ a_0 &= \frac{1}{3456q_e^{10}} \left(3e^{-\frac{2q_e}{\lambda_d}} k_c q_e c^2 + \frac{2h^2}{m} \right) \\ &\quad \times \left[\left(\frac{3e^{-\frac{2q_e}{\lambda_d}} k_c q_e (\lambda_d + q_e - 4e^{\frac{q_e}{\lambda_d}} (2\lambda_d + q_e)) c^2}{\lambda_d} + \frac{4h^2}{m} \right)^2 \right. \\ &\quad \left. - \left(\frac{3e^{-\frac{2q_e}{\lambda_d}} k_c q_e (\lambda_d + q_e) c^2}{\lambda_d} + \frac{5h^2}{m} \right)^2 \right]. \end{aligned}$$

The roots of the characteristic equation (which correspond to the eigenvalues of the linearized system) turn out to be quite complex to be easily analyzed. Instead of attempting to solve for the roots directly, we will use Descartes' rule of signs.

Fact 1 (Descartes' Rule of Signs) *Let $f(x) = a_n x^n + a_{n-1} x^{n-1} + \dots + a_1 x + a_0$ be a polynomial where a_n, a_{n-1}, \dots, a_0 are real coefficients. The number of positive real roots of f is either equal to the number of sign changes of successive terms of $f(x)$ or is less than that number by an even number (until 1 or 0 is reached). The number of negative real zeros of $f(x)$ is either equal to the number of sign changes of successive terms of $f(-x)$ or is less than that number by an even integer (until 1 or 0 is reached).*

Our strategy is to show that not all roots of $f(x)$ are negative real. If one of the roots of $f(x)$, χ , is not a negative real number, then $f(s^2)$ will have at least one eigenvalue with a positive real part, which is the square root of χ . If one eigenvalue of the linearized system has a positive real part, the unactuated nonlinear equations are then unstable. By way of contradiction, we will show that not all roots of $f(x)$ are negative.

Assume that all roots of $f(x)$ are negative. Then, by the Descartes rule of signs, we must have exactly three sign changes in the successive terms of $f(-x)$, which is given by

$$f(-x) = -a_3x^3 + a_2x^2 - a_1x + a_0.$$

Clearly we have $a_3 > 0$. So the first term in $f(-x)$ is negative. To ensure existence of 3 negative real roots, we need to have $a_2 > 0$, $a_1 > 0$ and $a_0 > 0$. In what follows, we will show that a_2 and a_0 can not both be positive.

First, lets rewrite a_2 in the form:

$$a_2 = \frac{e^{-2\beta} m \alpha}{72 q_e^2} (8e^{2\beta} h - 16e^\beta (\beta + 2) + 2\beta + 5),$$

where

$$\alpha = c^2 k_c m q_e \quad \beta = \frac{q_e}{\lambda_d} \quad \bar{h} = \frac{h^2}{\alpha}.$$

For a_2 to be positive, we must have

$$\bar{h} > \frac{1}{8e^{2\beta}} (16e^\beta (\beta + 2) - 2\beta - 5) = \kappa(\beta). \quad (22)$$

Note that $\kappa(\beta) > 0$ for all values of $\beta > 0$.

Next, we consider the expression for a_0 , which can be rewritten as:

$$a_0 = \frac{\alpha^3 (2\bar{h} + 3e^{-2\beta})}{3456 m^2 q_e^{10}} \left[(4\bar{h} + 3e^{-2\beta} (\beta - 4e^\beta (\beta + 2) + 1))^2 - (5\bar{h} + 3e^{-2\beta} (\beta + 1))^2 \right].$$

For a_0 to be positive, the expression in square brackets has to be positive. This expression is quadratic in \bar{h} , has two roots one negative and one positive. Let η denote the positive root. The negative root is of no concern to us because \bar{h} is positive. The positive root η is given by

$$\eta(\beta) = \frac{2}{3} e^{-2\beta} (2e^\beta \beta - \beta + 4e^\beta - 1).$$

Moreover, the quadratic term in square brackets has a negative hessian at the critical point. Hence, for a_0 is to be positive, we must have

$$\bar{h} < \eta. \quad (23)$$

One can verify that $\kappa > \eta$ for all $\beta \geq 0$ and, hence, inequalities (22) and (23) can not both be true. Hence a_2 and a_0 can not both be positive, which violates the necessary condition for having three negative real roots of $f(x)$. Thus, finally, there must exist a root χ that is either (1) positive real, or (2) complex with nonzero imaginary part. In both these cases, the square root of χ , which is a root of $f(s^2)$ and an eigenvalue of the linearized equations of motion, will have a positive real part. This concludes the proof that the linearized equations of motion are unstable and, hence, so are the full nonlinear equations of motion.

This instability is illustrated in the numerical simulation results shown in Fig. 3. The simulation time is 3 periods of the unperturbed solution. The numerical collinear invariant shape solution example of Hussein and Schaub (2006a) is used, but with the initial position vectors scaled by 0.1%. Without charge shielding the craft start to depart significantly from the equilibrium after one period. With the charge shielding present, the craft depart even quicker within 1 period.

Remark 3.1 (Stability of the Out-of-Plane Motion) *Note that the 3 spacecraft at any point in time form a plane. The initial angular momentum vector $\mathbf{J}_{\text{SO}(3)}(0)$ about the cluster center of mass uniquely defines the initial plane. However, it was shown above that the overall angular*

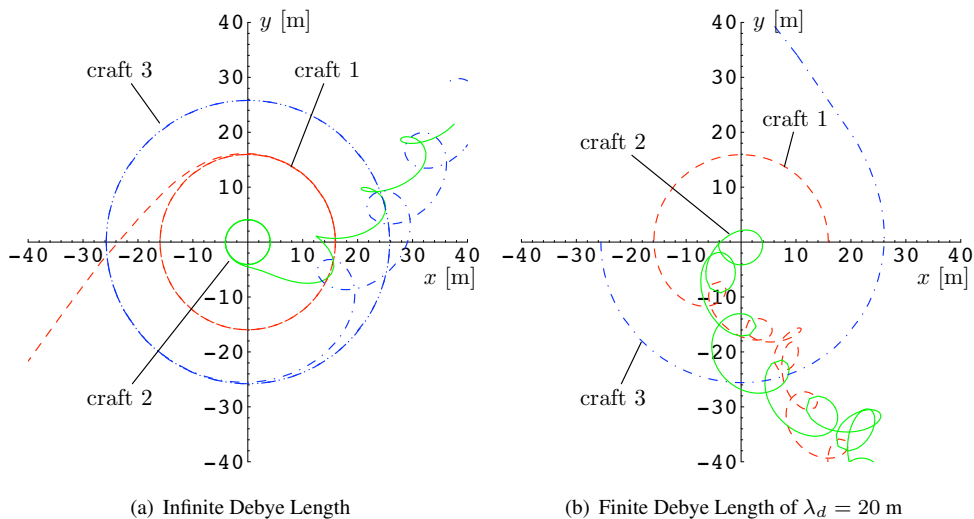


Fig. 3. Instability Illustration of Collinear Spinning Equilibrium with and without Plasma Charge Shielding

momentum $\mathbf{J}_{\text{SO}(3)}$ of the system is conserved. Hence, the common plane defined by the three craft remains fixed throughout the entire motion unless the system is acted upon by an external force. In the above analysis, we have essentially chosen the reference frame such that two of the frame axes lie within the orbital plane (as defined by the angular momentum) and the third is chosen as the normalized angular momentum vector $\mathbf{J}_{\text{SO}(3)}$. If the system experiences an impulsive out-of-plane small (and, hence, finite) perturbation force, the system angular momentum adjusts its direction, hence causing an overall acquired nonzero inclination i_0 from the original orbit. Hence, the out-of-plane motion is guaranteed to be bounded by the inclination angle i_0 . Thus, regardless of initial conditions, the out-of-plane angle inclination is guaranteed to be stable for the nonlinear system thanks to the conservation of angular momentum.

Remark 3.2 (General Nonsymmetric Case) Studying the stability of the general nonsymmetric three-craft Coulomb-tether problem is not very tractable in symbolic form. In this case, one can numerically study the stability of the open loop system. This will be investigated separately by the authors in the future. •

4. Stabilization

In this section we will use the linearized equations to design linear feedback control laws to locally stabilize the nonlinear system. We will follow a procedure similar to that of Sanyal et al. (2004) for physical tethers. We will first carry out a controllability test to determine whether all or some of the three charges need to be controlled to guarantee controllability of the linearized system. The control inputs are the charges c_1 , c_2 and c_3 . We will restrict the discussion to the symmetric formation case (equal masses and equal nominal charge magnitudes with equal separation distances). In linearizing the equations of motion we also have to linearize with respect to c_1 , c_2 and c_3 . With c_1 , c_2 and c_3 treated as control inputs in the fully-actuated case, the linearized equations of motion are

$$\mathbf{A}\delta\ddot{\mathbf{x}} + \mathbf{B}\delta\dot{\mathbf{x}} + \mathbf{C}\delta\mathbf{x} = \mathbf{D}\delta h + \mathbf{E}\delta\mathbf{c}. \quad (24)$$

where the matrices \mathbf{A} , \mathbf{B} , and \mathbf{C} are given in equations (20)-(20) and with

$$\mathbf{D} = \begin{bmatrix} \xi \\ q_e \\ \xi \\ q_e \\ 0 \end{bmatrix}$$

$$\mathbf{E} = \begin{bmatrix} \frac{mq_e\xi^2}{c_0} & -\frac{k_c c_0 e^{-\beta}}{q_e^2} & -\frac{k_c c_0 e^{-2\beta}}{4q_e^2} \\ -\frac{k_c c_0 e^{-2\beta}}{4q_e^2} & -\frac{k_c c_0 e^{-\beta}}{q_e^2} & \frac{mq_e\xi^2}{c_0} \\ 0 & 0 & 0 \end{bmatrix}$$

c_0 being the nominal spacecraft charging of craft 1 and 3, with craft 2 having a nominal charge of $-c_0$. In the above $\mathbf{c} = [c_1 \ c_2 \ c_3]^T$ is the control input. The parameter c_0 is free to be chosen, with the spin rate ξ found through Eq. (15):

$$\xi = \sqrt{\frac{c_0^2 k_c e^{-2\beta} (-1 + 4e^\beta)}{4mq_e^3}}. \quad (25)$$

The system is controllable using the controls c_1 , c_2 , and c_3 if and only if

$$\text{rank} \left([s^2 \mathbf{A} + s\mathbf{B} + \mathbf{C} \ \mathbf{E}] \right) = 3$$

holds for all eigenvalues s that satisfy $\det(s^2 \mathbf{A} + s\mathbf{B} + \mathbf{C}) = 0$ (Laub and Arnold, 1984; Sanyal et al., 2004). These eigenvalues are given in equation (20). Checking the controllability rank condition assuming all three charges are actuated, one finds that the rank is in fact 3 for all eigenvalues, which implies that the reduced equations of motion (i.e., shape dynamics) are controllable.

Note that any shape-stabilizing control law based on linear feedback control will guarantee stability of the motion even under perturbations in the spin rate ξ .

5. Numerical Simulations

The motion of three charged spacecraft in deep space is simulated numerically to illustrate the performance of the shape feedback control algorithm. These simulations assume a symmetric collinear setup where all craft have a mass of 50 kg, and a nominal separation distance of $q_{e1} = q_{e2} = 20$ meters. The equilibrium spacecraft charges are $c_{e1} = c_{e3} = 10\mu\text{C}$ and $c_{e2} = -10\mu\text{C}$. Two scenarios are tested with two different initial condition cases. The initial conditions for case 1 are described in Table 1. Here the initial separation distances are too large and the formation is not collinear. However, in case 1 the velocity magnitudes are chosen such that the actual angular momentum matches that of the equilibrium momentum.

The first stabilizing charge control is a simple linear PD control of the form

$$\delta \mathbf{c} = - \begin{bmatrix} \mathbf{K}_1 & \mathbf{K}_2 \end{bmatrix} \begin{bmatrix} \delta \mathbf{x} \\ \delta \dot{\mathbf{x}} \end{bmatrix} \quad (26)$$

State	Value	Units
$\mathbf{r}_1(t_0)$	(20.1, 0.0)	meters
$\mathbf{r}_2(t_0)$	(0.0, 0.0)	meters
$\mathbf{r}_3(t_0)$	(-19.0, 0.0)	meters
$\dot{\mathbf{r}}_1(t_0)$	(0, 0.022003)	meters/second
$\dot{\mathbf{r}}_2(t_0)$	(0, 0)	meters/second
$\dot{\mathbf{r}}_3(t_0)$	(0, -0.022003)	meters/second

Table 1
Initial Conditions for Simulation Case 1.

where \mathbf{K}_1 and \mathbf{K}_2 are the 3×3 proportional and derivative feedback gain matrices. For the presented simulations the feedback gain matrices are determined by solving the standard LQR gain selection problem with the weights of \mathbf{Q} defined as

$$\mathbf{Q} = \text{diag}(60, 60, 3600, 60, 60, 7200) \quad (27)$$

and \mathbf{R} being a 3×3 identity matrix scaled by 10^{11} .

Case 2 has identical simulation parameters as in case 1, but the initial velocity magnitudes are increased by 143% over those of case 1. This results in the actual angular momentum magnitude being different from the equilibrium momentum magnitude and $\delta H = 61.505 \text{ kg m}^2/\text{s}$. The linear stability analysis for this simulation case shows that the resulting motion will converge to the steady state tracking errors:

$$\delta \mathbf{x}_{\text{ss}} = (\mathbf{C} + \mathbf{E}\mathbf{K}_1)^{-1} \mathbf{D} \delta H = (0.62865 \text{ m}, 0.62865 \text{ m}, 0 \text{ rad})^T \quad (28)$$

The heading errors $\delta \theta_2$ are expected to converge to zero, with the separation distance errors $\delta \mathbf{q}_i$ reaching finite values.

While the closed loop stability is obtained using linearization results, all of the following numerical simulations integrate the full nonlinear equations of motion given by

$$m_i \ddot{\mathbf{r}}_i = \sum_{j=1, \neq i}^3 k_c c_i(t) c_j(t) \frac{\mathbf{r}_{ji}}{r_{ji}^3} e^{-\frac{r_{ji}}{\lambda_d}} \quad (29)$$

where \mathbf{r}_i are the inertial position vectors and $\mathbf{r}_{ji} = \mathbf{r}_i - \mathbf{r}_j$ are the relative position vectors.

The numerical results of case 1 are illustrated in Figure 4. The craft 2-D trajectories are illustrated in Figure 4(a) over a time span of 1.6231 hours, or 1 revolution of the un-perturbed problem. The shape tracking errors are shown in Figure 4(b) where initially both the separation distances q_1 and q_2 contain errors. With the charge feedback control active the 3-craft cluster shape assumes the desired collinear formation after about half a revolution. Furthermore, because δH is zero in this simulation setup, all shape tracking errors converge to zero over time. The spacecraft charges are illustrated in Figure 4(c). As the cluster converges to the desired spinning shape, the spacecraft charges converge to the equilibrium charges.

The numerical results of simulation case 2 are illustrated in Figure 5. Here the initial angular velocity magnitudes are increased by 143% such that $\delta H \neq 0$. With the linear PD control the spacecraft cluster still stabilizes its spinning motion about the desired collinear shape. However, the shape tracking errors δq_1 and δq_2 in Figure 5(b) do not converge to zero. The additional angular momentum causes the resulting shape to be too large. Or, the nominal charge are too weak to maintain a spinning formation at the desired shape. The offsets of the nonlinear simulation match

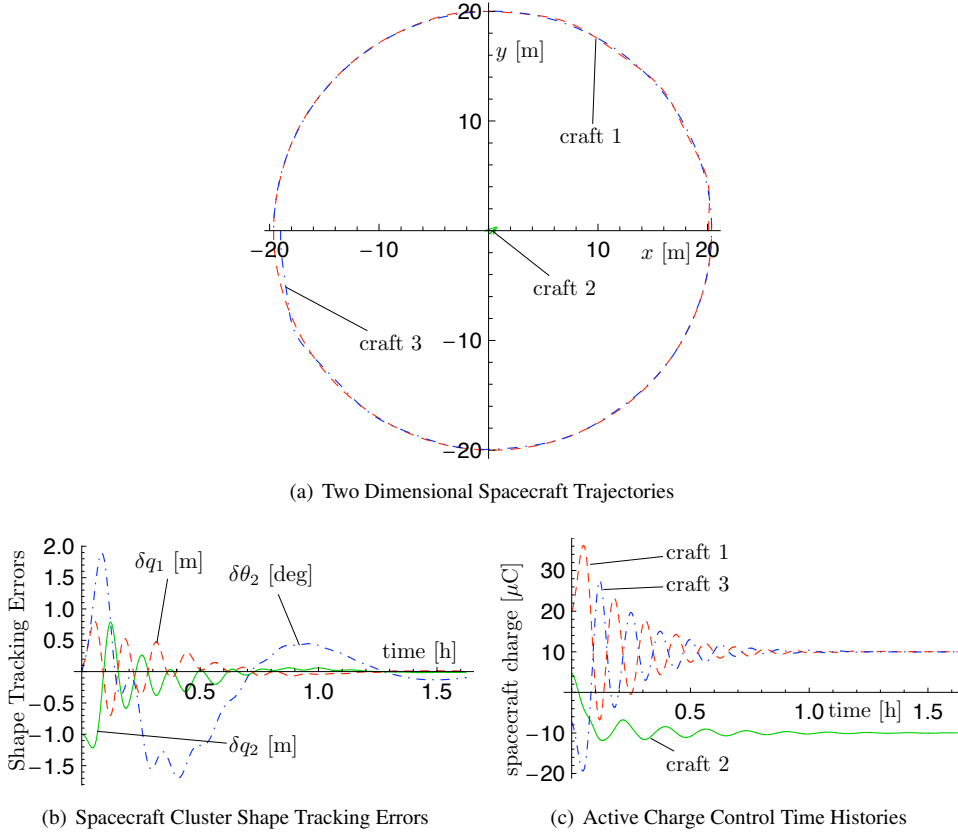


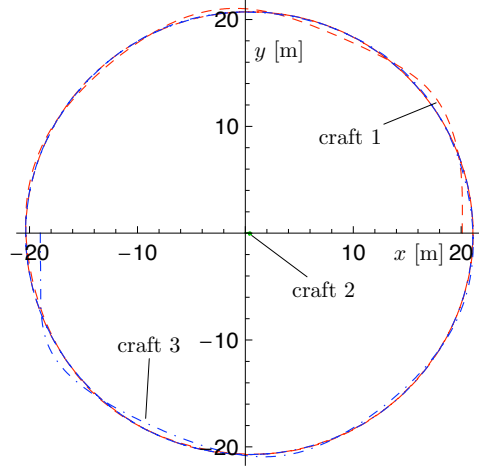
Fig. 4. Numerical Simulation Results of Linear PD Control with Case 1 where $\delta H = 0$.

up reasonably with the analytically predicted offsets of the linear stability analysis. The Debye shielding is causing enough of a nonlinearity to cause a small difference in predicted and actual offset. Note that even in this case the orientation error $\delta\theta_2$ converges to zero. Similarly the spacecraft charges shown in Figure 5(c) converge to a value different from the equilibrium charge. This difference is due to the persistent disturbance caused by the non-zero δH . This steady-state offsets to due momenta differences between actual and the desired equilibrium configuration could be compensated for with integral feedback.

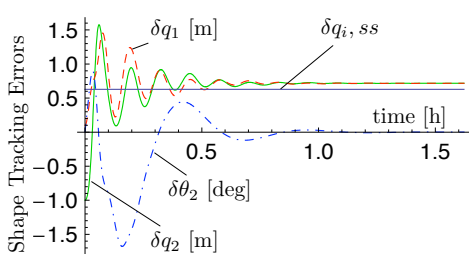
These steady-state offsets could be removed with the addition of integral feedback of the shape errors $\int\delta q_1$ and $\int\delta q_2$.

$$\delta \mathbf{c} = - \begin{bmatrix} \mathbf{K}_1 & \mathbf{K}_2 & \mathbf{K}_3 \end{bmatrix} \begin{bmatrix} \delta \mathbf{x} \\ \delta \dot{\mathbf{x}} \\ \left(\int \delta q_1 \right) \\ \left(\int \delta q_2 \right) \end{bmatrix} \quad (30)$$

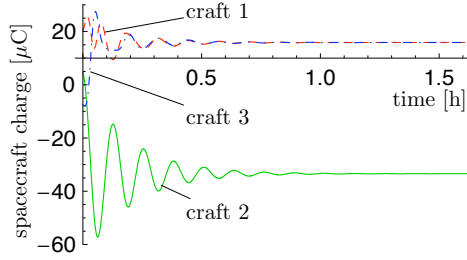
To select the feedback gains, the earlier \mathbf{Q} weight matrix is expanded to be defined as



(a) Two Dimensional Spacecraft Trajectories

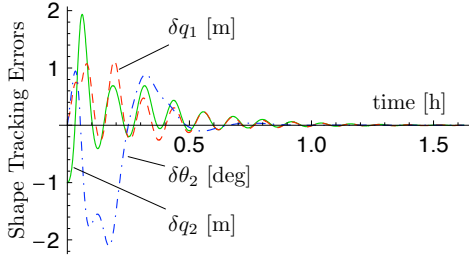


(b) Spacecraft Cluster Shape Tracking Errors

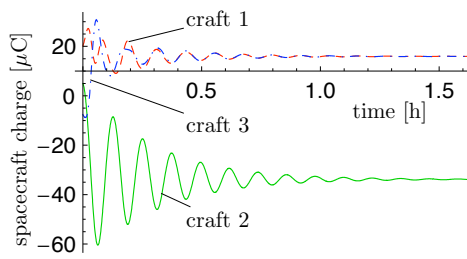


(c) Active Charge Control Time Histories

Fig. 5. Numerical Simulation Results of Linear PD Control with Case 2 where $\delta H \neq 0$.



(a) Spacecraft Cluster Shape Tracking Errors



(b) Active Charge Control Time Histories

Fig. 6. Numerical Simulation Results of Linear PID Control with Case 2 where $\delta H \neq 0$.

$$\mathbf{Q} = \text{diag}(60, 60, 3600, 60, 60, 7200, 0.0001, 0.0001) \quad (31)$$

Figure 6 shows the numerical simulation results using the case 2 initial conditions with a non-zero δH momentum difference. With the integral feedback added to the length errors, these shape errors now converge to zero as shown in Figure 6(a). The spacecraft charges shown in Figure 6(b) do not converge to the nominal design charge magnitude of $10 \mu\text{C}$. Instead they converge to larger values to compensate for the increased angular momentum of the system.

6. Conclusion

This paper studies the stability and control of relative equilibria for the three-craft Coulomb tether problem. General conditions are derived whose solutions are all relative equilibria for the spinning three-craft Coulomb tether constellation. Using linear feedback control theory, we stabilize the nonlinear system, guaranteeing that the system converges to a neighborhood of the desired relative equilibrium. Future research will focus on asymptotically stabilizing the desired relative equilibrium, regardless of the value of the angular momentum h . This will require the nominal equilibrium charge value to be changed to reflect the actual angular momentum of the system. We will also consider general nonlinear stabilization techniques, that may have larger regions of stability than linearization-based techniques considered in this paper.

References

- Berryman, J., Schaub, H., Aug. 7–11, 2005 2005a. Analytical charge analysis for 2- and 3-craft coulomb formations. In: AAS/AIAA Astrodynamics Specialists Conference. Lake Tahoe, CA, paper No. 05-278.
- Berryman, J., Schaub, H., Jan. 23–27 2005b. Static equilibrium configurations in GEO coulomb spacecraft formations. In: AAS Spaceflight Mechanics Meeting. Copper Mountain, CO, paper No. AAS 05–104.
- Escoubet, C. P., Fehringer, M., Goldstein, M., 2001. The cluster mission. *Annales Geophysicae* 19 (10/12), 1197–1200.
- Gombosi, T. I., 1998. *Physics of the Space Environment*. Cambridge University Press, New York, NY.
- Hussein, I. I., Schaub, H., January 22–26 2006a. Invariant shape solutions of the spinning three craft coulomb tether problem. In: AAS Space Flight Mechanics Meeting. Tampa, Florida, paper No. AAS 06-228.
- Hussein, I. I., Schaub, H., 2006b. Invariant shape solutions of the spinning three craft coulomb tether problem. *Celestial Mechanics and Dynamical Astronomy* 96, 137–157.
- King, L. B., Parker, G. G., Deshmukh, S., Chong, J.-H., January 2002. Spacecraft formation-flying using inter-vehicle coulomb forces. Tech. rep., NASA/NIAC, <http://www.niac.usra.edu>.
- King, L. B., Parker, G. G., Deshmukh, S., Chong, J.-H., May–June 2003. Study of interspacecraft coulomb forces and implications for formation flying. *AIAA Journal of Propulsion and Power* 19 (3), 497–505.
- Lappas, V., Saaj, C., Richie, D., Peck, M., Streeman, B., Schaub, H., Jan. 28–Feb. 1 2007. Spacecraft formation flying and reconfiguration with electrostatic forces. In: AAS/AIAA Space Flight Mechanics Meeting. Sedona, AZ, Paper AAS 07–113.
- Laub, A. J., Arnold, W. F., February 1984. Controllability and observability criteria for multivariable linear second-order models. *IEEE Transactions on Automatic Control* AC-29 (2), 163–165.
- Marsden, J. E., 1992. *Lectures on Mechanics*. Cambridge University Press, Cambridge.
- Marsden, J. E., Ratiu, T. S., 1999. *Introduction to Mechanics and Symmetry*. Springer-Verlag, New York, NY.
- Mullen, E. G., Gussenhoven, M. S., Hardy, D. A., A. Aggson, T., Ledley, B. G., 1986. Scatha survey of high-voltage spacecraft charging in sunlight. *Journal of the Geophysical Sciences*

- 91 (A2), 1474–1490.
- Natarajan, A., Schaub, H., July–Aug. 2006. Linear dynamics and stability analysis of a coulomb tether formation. *Journal of Guidance, Control, and Dynamics* 29 (4), 831–839.
- Natarajan, A., Schaub, H., Jan. 28–Feb. 1 2007. Hybrid control of orbit normal and along-track 2-craft coulomb tethers. In: *AAS Space Flight Mechanics Meeting*. Sedona, AZ, Paper AAS 07–193.
- Natarajan, A., Schaub, H., Parker, G. G., Jan. 22–26 2006. Reconfiguration of a 2-craft coulomb tether. In: *AAS Space Flight Mechanics Meeting*. Tampa, FL, paper No. AAS-06-229.
- Nicholson, D. R., 1992. *Introduction to Plasma Theory*. Krieger, Malabar, FL.
- Romanelli, C. C., Natarajan, A., Schaub, H., Parker, G. G., King, L. B., Jan. 22–26 2006. Coulomb spacecraft voltage study due to differential orbital perturbations. In: *AAS Space Flight Mechanics Meeting*. Tampa, FL, paper No. AAS-06-123.
- Sanyal, A. K., Shen, J., McClamroch, N. H., 2004. Control of a dumbbell spacecraft using attitude and shape control inputs only. In: *Proceedings of the American Control Conference*. Boston, MA, pp. 1014–1018.
- Schaub, H., Hall, C., Berryman, J., June 12–15 2005. Necessary conditions for circularly-restricted static coulomb formations. In: *AAS Malcolm D. Shuster Astronautics Symposium*. Buffalo, NY, paper No. AAS 05–472.
- Schaub, H., Hussein, I. I., 3 2007. Stability and reconfiguration analysis of a circularly spinning 2-craft coulomb tether. In: *2007 IEEE Aerospace Conference*. Big Sky, MT.
- Schaub, H., Parker, G. G., King, L. B., Jan.–June 2004. Challenges and prospect of coulomb formations. *Journal of the Astronautical Sciences* 52 (1–2), 169–193.
- Torkar, K., et. al., 1999. Spacecraft potential control aboard equator-s as a test for cluster-ii. *Annales Geophysicae* 17, 1582–1591.
- Whipple, E. C., Olsen, R. C., Nov. 12–14 1980. Importance of differential charging for controlling both natural and induced vehicle potentials on ats-5 and ats-6. In: *Proceedings of the 3rd Spacecraft Charging Technology Conference*. p. 887, nASA Conference Publication 2182.

Appendix: Linearized Collinear Relative Equations of Motion

In Eq. (18) the linearized equations of motion for the collinear equilibrium condition are given as:

$$\mathbf{A}\delta\ddot{\mathbf{x}} + \mathbf{B}\delta\dot{\mathbf{x}} + \mathbf{C}\delta\mathbf{x} = 0$$

The matrices \mathbf{A} , \mathbf{B} , \mathbf{C} and \mathbf{D} are as follows:

$$\mathbf{A} = \begin{bmatrix} \frac{m_1(m_2 + m_3)}{M} & \frac{m_1 m_3}{M} & 0 \\ \frac{m_1 m_3}{M} & \frac{(m_1 + m_2)m_3}{M} & 0 \\ 0 & 0 & \frac{m_1 m_2 m_3 q_{e1}^2 q_{e2}^2}{m_2 m_3 q_{e2}^2 + m_1 (m_2 q_{e1}^2 + m_3 (q_{e1} + q_{e2})^2)} \end{bmatrix}$$

$$\mathbf{B} = \frac{1}{m_2 m_3 q_{e2}^2 + m_1 (m_2 q_{e1}^2 + m_3 (q_{e1} + q_{e2})^2)} \times \begin{bmatrix} 0 & 0 & 2m_1 m_2 m_3 q_{e1} q_{e2}^2 \xi \\ 0 & 0 & -(2m_1 m_2 m_3 q_{e1}^2 q_{e2} \xi) \\ -(2m_1 m_2 m_3 q_{e1} q_{e2}^2 \xi) & 2m_1 m_2 m_3 q_{e1}^2 q_{e2} \xi & 0 \end{bmatrix}$$

$$\mathbf{C} = \begin{bmatrix} C_{11} & C_{12} & C_{13} \\ C_{21} & C_{22} & C_{23} \\ C_{31} & C_{32} & C_{33} \end{bmatrix}$$

$$\mathbf{D} = \begin{bmatrix} \frac{2m_1(m_2 q_{e1} + m_3(q_{e1} + q_{e2}))\xi}{m_2 m_3 q_{e2}^2 + m_1 (m_2 q_{e1}^2 + m_3 (q_{e1} + q_{e2})^2)} \\ \frac{2m_3(m_2 q_{e2} + m_1(q_{e1} + q_{e2}))\xi}{m_2 m_3 q_{e2}^2 + m_1 (m_2 q_{e1}^2 + m_3 (q_{e1} + q_{e2})^2)} \\ 0 \end{bmatrix}$$

The matrix coefficients of \mathbf{C} are given by:

$$\begin{aligned}
C_{11} &= \frac{1}{\lambda_d q_{e1}^3 (q_{e1} + q_{e2})} \times \\
&\frac{1}{\left(c_1 m_2 (m_1 q_{e1} - m_3 q_{e2}) q_{e2}^2 + c_2 e^{\frac{q_{e1}}{\lambda_d}} m_1 (q_{e1} + q_{e2})^2 (m_2 q_{e1} + m_3 (q_{e1} + q_{e2})) \right)} \times \\
&\frac{1}{(m_2 m_3 q_{e2}^2 + m_1 (m_2 q_{e1}^2 + m_3 (q_{e1} + q_{e2})^2))} \times \\
&c_1 c_2 e^{-\frac{q_{e1}}{\lambda_d}} k_c \left(c_2 e^{\frac{q_{e1}}{\lambda_d}} m_1 \left(\lambda_d \left(-m_1 (m_2 + m_3)^2 q_{e1}^3 + 3(m_1 + m_2) m_3 (m_2 + m_3) q_{e2}^2 q_{e1} \right. \right. \right. \\
&\left. \left. \left. + 2(m_1 + m_2) m_3^2 q_{e2}^3 \right) \right. \right. \\
&\left. \left. + q_{e1} (m_2 q_{e1} + m_3 (q_{e1} + q_{e2})) (m_2 m_3 q_{e2}^2 + m_1 (m_2 q_{e1}^2 + m_3 (q_{e1} + q_{e2})^2)) \right) (q_{e1} + q_{e2})^3 \right. \\
&\left. + c_1 q_{e2}^2 \left(m_1 q_{e1} (q_{e1} + q_{e2}) (m_2 q_{e1} + m_3 (q_{e1} + q_{e2})) (m_2 m_3 q_{e2}^2 + m_1 (m_2 q_{e1}^2 + m_3 (q_{e1} + q_{e2})^2)) \right. \right. \\
&\left. \left. + \lambda_d \left(-2m_2^2 m_3^2 q_{e2}^4 + m_1 m_2 m_3 (m_3 (q_{e1} - 2q_{e2}) (q_{e1} + q_{e2}) + m_2 q_{e1} (q_{e1} + 3q_{e2})) q_{e2}^2 \right. \right. \right. \\
&\left. \left. \left. - m_1^2 q_{e1} (q_{e1} + q_{e2}) \left((m_2 + m_3)^2 q_{e1}^2 + 2m_3 (m_2 + m_3) q_{e2} q_{e1} + m_3 (m_3 - 3m_2) q_{e2}^2 \right) \right) \right) \right)
\end{aligned}$$

$$\begin{aligned}
C_{22} = & \frac{1}{q_{e1}^2 \left(c_1 m_2 (m_1 q_{e1} - m_3 q_{e2}) q_{e2}^2 + c_2 e^{\frac{q_{e1}}{\lambda_d}} m_1 (q_{e1} + q_{e2})^2 (m_2 q_{e1} + m_3 (q_{e1} + q_{e2})) \right)} \times \\
& c_1 c_2 k_c m_3 \left(\frac{c_1 e^{-\frac{q_{e1}}{\lambda_d}} (m_2 q_{e2} + m_1 (q_{e1} + q_{e2})) q_{e2}^2}{\lambda_d} \right. \\
& + \frac{2c_1 e^{-\frac{q_{e1}}{\lambda_d}} (m_2 q_{e2} + m_1 (q_{e1} + q_{e2})) q_{e2}^2}{q_{e1} + q_{e2}} + \frac{c_2 (q_{e1} + q_{e2})^2 (m_2 q_{e2} + m_1 (q_{e1} + q_{e2}))}{\lambda_d} \\
& + (m_1 + m_2) \left(c_1 e^{-\frac{q_{e1}}{\lambda_d}} q_{e2}^2 + c_2 (q_{e1} + q_{e2})^2 \right) \\
& \left. - \frac{4e^{-\frac{q_{e1}}{\lambda_d}} m_3 (m_2 q_{e2} + m_1 (q_{e1} + q_{e2}))^2 \left(c_1 q_{e2}^2 + c_2 e^{\frac{q_{e1}}{\lambda_d}} (q_{e1} + q_{e2})^2 \right)}{m_2 m_3 q_{e2}^2 + m_1 (m_2 q_{e1}^2 + m_3 (q_{e1} + q_{e2})^2)} \right. \\
& \left. + \frac{2c_2 (q_{e1} + q_{e2})^2 (m_2 q_{e2} + m_1 (q_{e1} + q_{e2}))}{q_{e2}} \right)
\end{aligned}$$

$$\begin{aligned}
C_{33} = & \frac{1}{q_{e1} (q_{e1} + q_{e2})} \times \\
& \frac{1}{\left(c_1 m_2 (m_1 q_{e1} - m_3 q_{e2}) q_{e2}^2 + c_2 e^{\frac{q_{e1}}{\lambda_d}} m_1 (q_{e1} + q_{e2})^2 (m_2 q_{e1} + m_3 (q_{e1} + q_{e2})) \right)} \times \\
& c_1 c_2 e^{-\frac{q_{e1}}{\lambda_d}} k_c m_3 q_{e2} \left(c_1 m_2 q_{e2}^3 - c_2 e^{\frac{q_{e1}}{\lambda_d}} m_1 (q_{e1} + q_{e2})^3 \right)
\end{aligned}$$

$$\begin{aligned}
C_{12} = & \frac{1}{q_{e1}^2 \left(c_1 m_2 (m_1 q_{e1} - m_3 q_{e2}) q_{e2}^2 + c_2 e^{\frac{q_{e1}}{\lambda_d}} m_1 (q_{e1} + q_{e2})^2 (m_2 q_{e1} + m_3 (q_{e1} + q_{e2})) \right)} \times \\
& c_1 c_2 e^{-\frac{q_{e1}}{\lambda_d}} k_c m_3 \left(\frac{c_1 (m_2 q_{e2} + m_1 (q_{e1} + q_{e2})) q_{e2}^2}{\lambda_d} + \frac{2c_1 (m_2 q_{e2} + m_1 (q_{e1} + q_{e2})) q_{e2}^2}{q_{e1} + q_{e2}} \right. \\
& + m_1 \left(c_1 q_{e2}^2 + c_2 e^{\frac{q_{e1}}{\lambda_d}} (q_{e1} + q_{e2})^2 \right) \\
& \left. - \frac{4m_1 (m_2 q_{e2} + m_1 (q_{e1} + q_{e2})) (m_2 q_{e1} + m_3 (q_{e1} + q_{e2})) \left(c_1 q_{e2}^2 + c_2 e^{\frac{q_{e1}}{\lambda_d}} (q_{e1} + q_{e2})^2 \right)}{m_2 m_3 q_{e2}^2 + m_1 (m_2 q_{e1}^2 + m_3 (q_{e1} + q_{e2})^2)} \right)
\end{aligned}$$

$$\begin{aligned}
C_{12} &= C_{21} \\
C_{13} &= C_{31} = 0 \\
C_{23} &= C_{32} = 0
\end{aligned}$$